

Inductance of tubular rectangular high current busduct of finite length

Abstract. The study attempts to calculate the mutual inductance busbar rectangular profile leading sinusoidal alternating current, to operate the internal coil of an induction heater. The results of these calculations have been compared with simulation in the FEMM program ver. 4.2. The input impedance of wire track is defined as the ratio of voltage to current. The analysis was conducted for inductor current frequencies of 9835 Hz, taking into account the phenomenon of skin effect and the effect of approximation.

Streszczenie. W pracy podjęto próbę obliczenia indukcyjności wzajemnej przewodów szynowych o profilu prostokątnym wiodących prąd sinusoidalnie zmienny, służących do zasilania wzbudnika wewnętrznego układu nagrzewnicy indukcyjnej. Wyniki tych obliczeń porównano z symulacją komputerową w programie FEMM ver. 4.2., gdzie impedancja wejściowa szynoprzewodu określona jest jako stosunek napięcia do prądu. Analizę przeprowadzono dla częstotliwości prądu wzbudnika 9835 Hz, uwzględniając zjawisko naskórkowości oraz efekt zbliżenia. (Indukcyjność rurowego prostokątnego toru wielkoprądowego o skończonej długości).

Słowa kluczowe: Pole elektromagnetyczne, nagrzewanie indukcyjne, hartowanie indukcyjne, naskórkowość.

Keywords: Electromagnetic field, induction heating, induction hardening, skin effect.

Introduction

Single-phase transfer line for medium and high frequencies, created by the rails of the rectangular profile is one of the solutions to the power inductor in the process of induction heating of metals [1-7]. An example of such a system is a power inductor for induction hardening of the internal piping loads [8-11] presented in Figure 1

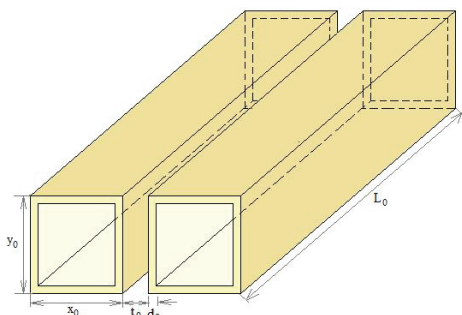


Fig.1. A busbar of pipes rectangular cross-section

Because of the medium and high frequency current in the power circuit inductor busbars is important in the distribution of the electromagnetic field play a skin effect and proximity phenomena. These phenomena give rise to uneven distribution of current density and magnetic field in busbars, which in turn significantly influence the size of losses in the track, the temperature distribution, electrodynamic force between the wires and the replacement of the transmission line parameters [6, 12-20]. Distribution of current density and magnetic field in the vicinity of the tubular high current busducts and without taking into account skin effect and proximity effects, and its electrical parameters was determined in many works of analytical methods, numerical and analytical-numerical characters for the use of rectangular busbars in power [19, 21-27]. However, in the work of these and other busbar shall be extended, allowing you consider the electromagnetic field in a 2D system. In the works [28-32] was determined and the impedance of the magnetic field of a single wire track of the rectangular profile and finite length but, assuming even distribution of power. In this article, therefore, made an attempt to develop algorithms and methods for determining the electromagnetic field in a

single phase circuit of high current busducts of rectangular finite length, and taking into account the phenomena of skin effect and proximity. Used on various algorithms are described, inter alia, in [9, 11, 33], which is implemented in a computer program written in C #, object-oriented. Built a class program and includes a number of methods to further its expansion to the analysis of induction heating systems also take into account Inductor and work piece 1. The calculation results were compared with the simulations system made generally available in the FEMM program ver. 4.2

Illustrative example

Set is a system of two straight wires of length l , rectangular with sides b , h , l the thickness, electrical conductivity γ , made of a material with magnetic permeability μ_0 non ferromagnetics here (Fig. 1). Let between the ends of these wires are forced sinusoidally time-varying potential differences in the pulsation ω whose values are complex, \underline{U}_1 and \underline{U}_2 (Fig. 2).

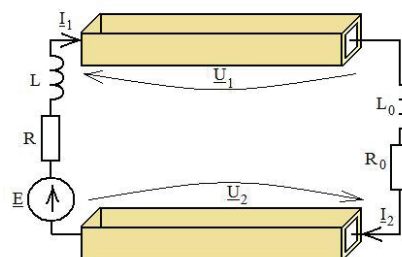


Fig.2. Induction heating diagram: \underline{E}, R, L - power source inside parameters, R_0, L_0 – work piece and inductor parameters.

Forced in this way the electric field inside the pipe – $\text{grad} \underline{V}(X)$ causes the rate of flow of a current density of the complex $\underline{J}(X)$, which in turn induces the wires inside and outside the complex electric field induction equal $-\underline{j}\omega \underline{A}(X)$. Resultant complex electric field then takes the form [34]:

$$(1) \quad \underline{E}(X) = -\text{grad} V(X) - j\omega \underline{A}(X)$$

where the composite magnetic vector potential

$$(2) \quad \underline{A}(x_1, x_2, x_3) = \frac{\mu_0}{2\pi} \cdot \sum_{p=1}^2 \int_{v^{(p)}} \frac{\underline{J}(y_1, y_2, y_3)}{\sqrt{(x_1 - y_1)^2 + (x_2 - y_2)^2 + (x_3 - y_3)^2}} dy_1 dy_2 dy_3$$

where $v^{(p)}$ is an area in which the p-th conductor. Taking into account Ohm's law

$$(3) \quad \underline{J}(x_1, x_2, x_3) = \sigma \underline{E}(x_1, x_2, x_3)$$

and equation (7) and (8), obtained by the equation

$$(4) \quad -\text{grad} V(x_1, x_2, x_3) = \frac{1}{\sigma} \underline{J}(x_1, x_2, x_3) + j \frac{\omega \mu_0}{2\pi} \cdot \sum_{p=1}^2 \int_{v^{(p)}} \frac{\underline{J}(y_1, y_2, y_3)}{\sqrt{(x_1 - y_1)^2 + (x_2 - y_2)^2 + (x_3 - y_3)^2}} dy_1 dy_2 dy_3$$

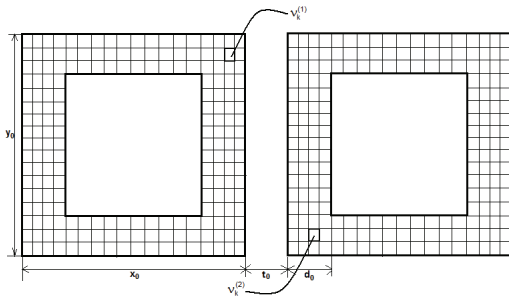


Fig. 3. Breakdown of the elements of the cable

Then, the division shall be calculated on the area as the rectangular fibers in Figure 3.

It is assumed that each fiber along the total current is constant and denoted $\underline{I}_k^{(p)}$. Denote the area of k-fiber, p-cable to the $v_k^{(p)}$. In the area of fiber $v_k^{(p)}$ vector current density can be approximated as follows:

$$(5) \quad \underline{J}(x_1, x_2, x_3) \Big|_{(x_1, x_2, x_3) \in v_k^{(p)}} = \frac{I_k^{(p)}}{\Delta S} \bar{\mathbf{1}}_{x_3}$$

where $\bar{\mathbf{1}}_{x_3}$ - unit vector in the direction of the axis x_3

If the integral equation (4) substituting approximation (5), the integral in the areas $v^{(1)}$, $v^{(2)}$ express as the sum of integrals of the fibers $v_k^{(p)}$, and multiply by a vector $\frac{1}{\Delta S} \bar{\mathbf{1}}_{x_3}$,

and then calculate the integral to any fiber $v_k^{(s)}$ shall then:

$$R_n^{(s)} \underline{I}_n^{(s)} + j\omega \sum_{p=1}^2 \sum_{k=1}^N (-1)^{s+p} M_{n,k}(s,p) \underline{I}_k^{(p)} = \underline{U}_n^{(s)}$$

(6)

$$(s = 1, 2)(n = 1, 2, \dots, N)$$

where N- the number of fibers in the wire. From Eq. (6) we have

(11)

(7)

$$R_n^{(s)} \underline{I}_n^{(s)} = \int_{v_n^{(s)}} \frac{1}{\sigma} \underline{J}(x_1, x_2, x_3) \frac{\bar{\mathbf{1}}_{x_3}}{\Delta S} dx_1 dx_2 dx_3 = \frac{l}{\sigma \Delta S} \underline{I}_n^{(s)}$$

where the resistance of fiber to fiber n-s-the wire

$$(8) \quad R_n^{(s)} = \frac{l}{\sigma \Delta S}$$

and the mutual inductance

(9)

$$M_{n,k}^{(s,p)} = \frac{\mu_0}{2\pi} \frac{1}{(\Delta S)^2} \int_{v^{(p)}} \frac{dx_3 dx_2 dx_1 dy_3 dy_2 dy_1}{\sqrt{(x_1 - y_1)^2 + (x_2 - y_2)^2 + (x_3 - y_3)^2}}$$

The coefficients $M_{n,k}^{(s,p)}$ expressed sixfold integral can be expressed analytically. This is especially important in cases where $v_k^{(s)} = v_k^{(p)}$ because then the integral is improper integral and the numerical calculation would then be difficult. The coefficients $M_{n,k}^{(s,p)}$ expressed integral (9) coefficients can be interpreted as inductivity two fibers $v_k^{(s)}$ and $v_k^{(p)}$.

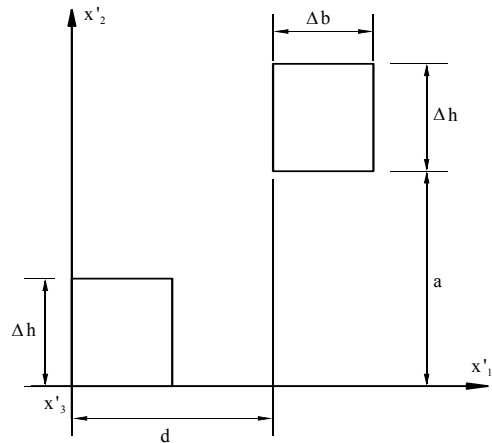


Fig. 4 Determination of the parameters defining the position of the two fibers to each other

Assuming the sign to identify the location of the two fibers to each other as in Figure 4, six-time integral (9) can be expressed as a function of $M(l, \Delta b, \Delta h, d, a)$ parameters, l - length of the cord, Δb , Δh - the dimensions of the transverse fibers, d, and - the distance between the fibers along the axis, respectively x'_1 and x'_2

(10)

$$M(l, \Delta b, \Delta h, d, a) = \frac{\mu_0}{2\pi} \frac{1}{(\Delta b \Delta h)^2} \cdot$$

$$\int_0^l \int_0^{\Delta h} \int_0^{\Delta b} \int_0^l \int_a^{a+\Delta h} \int_d^{d+\Delta b} \frac{dx_3 dx_2 dx_1 dy_3 dy_2 dy_1}{\sqrt{(x_1 - y_1)^2 + (x_2 - y_2)^2 + (x_3 - y_3)^2}}$$

Function (10) as a function of five variables borders sixfold integration is analytical form. After a complicated integrations the simplistic assumption of a single $l^2 \gg d^2 + a^2$ demonstrated that it has the following form (11):

$$M(l, \Delta b, \Delta h, d, a) = \frac{\mu_o}{2\pi} \frac{1}{(\Delta b \Delta h)^2} \int_0^l \int_0^{\Delta h} \int_0^{\Delta b} \int_0^{a+\Delta h} \int_0^{d+\Delta b} \frac{dx_3 dx_2 dx_1 dy_2 dy_1}{\sqrt{(x_1 - y_1)^2 + (x_2 - y_2)^2 + (x_3 - y_3)^2}} =$$

$$= \frac{\mu_o \cdot l}{2\pi} \left[\ln(2l) + \frac{13}{12} + \frac{1}{(\Delta b \Delta h)^2} \cdot \left[\begin{aligned} & -\frac{1}{2} f_1(d + \Delta b, a) - \frac{1}{2} f_1(d - \Delta b, a) + f_1(d, a) + \frac{1}{4} f_1(d + \Delta b, a - \Delta h) + \frac{1}{4} f_1(d - \Delta b, a - \Delta h) \\ & - \frac{1}{2} f_1(d, a - \Delta h) + \frac{1}{4} f_1(d + \Delta b, a + \Delta h) + \frac{1}{4} f_1(d - \Delta b, a + \Delta h) - \frac{1}{2} f_1(d, a + \Delta h) \\ & + f_2(a, d + \Delta b) + f_2(a, d - \Delta b) - 2f_2(a, d) - \frac{1}{2} f_2(a - \Delta h, d + \Delta b) - \frac{1}{2} f_2(a - \Delta h, d - \Delta b) \\ & + f_2(a - \Delta h, d) - \frac{1}{2} f_2(a + \Delta h, d + \Delta b) - \frac{1}{2} f_2(a + \Delta h, d - \Delta b) + f_2(a + \Delta h, d) \end{aligned} \right] \right]$$

where

$$(12) f_1(x, y) = \left(\frac{1}{12} x^4 - \frac{1}{2} x^2 y^2 + \frac{1}{12} y^4 \right) \ln|x^2 + y^2|$$

$$(13) f_2(x, y) = \frac{1}{3} x^3 y \operatorname{arctg}\left(\frac{y}{x}\right) + \frac{1}{3} x y^3 \operatorname{arctg}\left(\frac{x}{y}\right).$$

If $a = 0$ and $b = 0$, ie when the overlap integral of the fibers (9) becomes the integral improper but convergent, and can then be made in the formula (11) border crossing as a result of which is obtained:

$$L(l, \Delta b, \Delta h) = \lim_{\substack{d \rightarrow 0 \\ a \rightarrow 0}} M(l, \Delta b, \Delta h, d, a) =$$

$$(14) \frac{\mu_o l}{2\pi} \left[\ln(2l) + \frac{13}{12} - \frac{1}{2} \ln|(\Delta b)^2 + (\Delta h)^2| + \right.$$

$$\left. + \frac{1}{12} \left(\frac{\Delta b}{\Delta h} \right)^2 \ln \left| 1 + \left(\frac{\Delta h}{\Delta b} \right)^2 \right| + \frac{1}{12} \left(\frac{\Delta h}{\Delta b} \right)^2 \ln \left| 1 + \left(\frac{\Delta b}{\Delta h} \right)^2 \right| - \right.$$

$$\left. - \frac{2}{3} \frac{\Delta b}{\Delta h} \operatorname{arctg}\left(\frac{\Delta h}{\Delta b}\right) - \frac{2}{3} \frac{\Delta h}{\Delta b} \operatorname{arctg}\left(\frac{\Delta b}{\Delta h}\right) \right]$$

Formula (13) can be interpreted as the coefficient of self induction fibers with rectangular and the length l .

Exemplary calculations and computation results

As marked on Figure 1, the following dimensions of rectangular wires: $x_0 = 20$ mm, $y_0 = 25$ mm, wall thickness of the rectangular profile $t_0 = 2$ mm, profile length $L = 2$ m. The distance between conductors is $d_0 = 2$ mm. Supply voltage frequency is 9835 Hz. Assumed that the cable is made of copper with a relative permeability $\mu_r = 1$, and conductivity of $\sigma = 5.6 \cdot 10^7$ S/m. Party leading applications developed in C # implemented in Microsoft Visual Studio ver. 8.0 is shown in Figure 3.

In Figure 3 it is also shown $Z = 2,589 + j16,525[m\Omega]$, the value of imaginary impedance value of which corresponds to the inductive reactance and amounts $X_L = 16,525 [m\Omega]$.

Inductance $L = X_L / 2\pi f$ is calculated for a frequency $f = 9835$ Hz is $0.27 \mu H$.

In multi-variant FEMM simulations were performed for different geometries busway. For the discretization using triangular elements with linear approximation. The grid was generated independently for the busway and the surrounding airspace and consisted of 48,361 nodes and 96,686 Elements. For border areas used as Dirichlet boundary conditions in Figure 4.

Foster impedance test system consisting of two rail lines was calculated as the ratio doubled to the current and voltage is $Z = 2,785 + j17,037[m\Omega]$, the impedance obtained in the program is C # and is lower by about 5% of the estimated impedance in FEMM.

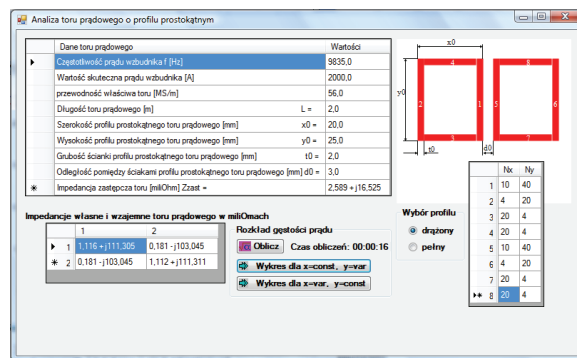


Fig. 3 Front Page Visual C #

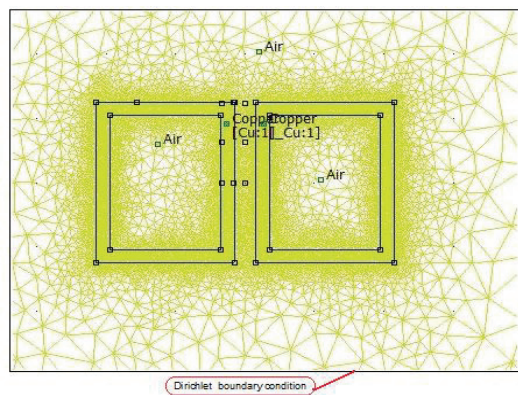


Fig. 4 Two-dimensional model of wire track with a visible grid

The results of calculations for a single rectangular profile FEMM for $f = 9835$ Hz

Circuit Properties	
Results	FEMM Output
Total current = 2000 Amps	Title: TOR-2010-BB-kwadrat
Voltage Drop = 2.78521+I*17.0378 Volts	Length Units: Millimeters
Flux Linkage = 0.000275714-I*4.78836e-007 Webers	2-D Planar (Depth: 2000 mm)
Flux/Current = 1.37857e-007-I*2.39418e-010 Henries	Frequency: 9835 Hz
Voltage/Current = 0.0013926+I*0.00851891 Ohms	48361 Nodes
Real Power = 2785.21 Watts	96686 Elements
Reactive Power = 17037.8 VAR	
Apparent Power = 17264 VA	

Fig. 5 The results of calculations for a single rectangular profile FEMM for $f = 9835$ Hz

Conclusion

Algorithm studies because of the number of fibers N , but found no oscillations in the distribution of the $N = 600$ th application in C # allows you to easily change system parameters such as the frequency or length of the cables, as well as geometric dimensions. Performed simulations show that the program FEMM is a useful tool for preliminary and approximate analysis of the magnetic field. Using this program, a computer simulation was carried out multi-variant changes in the value of current, or frequency, or length of the track. There is also an opportunity to modify the geometrical dimensions of the track, but it requires drawing a cross over again. For different frequency compared to the value of source inductance of the input received in C # with inductance calculated in FEMM while at work, the results for a frequency of 9835 Hz. These results differ less than 5%.

This work was partly financed by the Polish Ministry of Science and Higher Education from means of budget on science in years 2010-2012 as research project N N510 256338.

REFERENCES

- [1] Hering M.: *Podstawy elektrotermii. Część II*. WNT, Warszawa 1998.
- [2] Langer E.: *Teorie indukčního a dielektrického tepla*. Academia, Praha 1979.
- [3] Davies E.J.: *Conduction and Induction Heating*. Peter Peregrinus Ltd., London 1990.
- [4] Sajdak C., Samek E.: *Nagrzewanie indukcyjne. Podstawy teoretyczne i zastosowania*. Wyd. Śląsk, Katowice 1987.
- [5] Barglik J., Muszyński J.: *Stanowisko do hartowania indukcyjnego rur wzbudnikiem wewnętrznym*. Materiały konferencji „Badania naukowe w elektrotermii”. Wiśła 1988 r. ss. 12-19.
- [6] Rudnev V., Loveless D., Cook R., Black M.: *Handbook of Induction Heating*. Copyright by Marcel Dekker, New York 2003.
- [7] Barglik J., Doležel I., Karban P., Kwiecień I., Ulrych B.: *Comparison of two ways of induction hardening of long steel tubes*. Proceedings of the XIII International Symposium on Theoretical Electrical Engineering. ISET'05 Lvov 2005 pp. 11-14.
- [8] Piątek Z., Doležel I., Baron B.: *Pole magnetyczne we wsadzie rurowym nagrzewanym indukcyjnie od wewnątrz*. Przegląd Elektrotechniczny, Rok LXXXI, No. 6, 2005, 48-51.
- [9] Baron B., Kolańska-Płuska J., Krych J.: *Application of Bessel functions and discrete Fourier transform to the analysis of electromagnetic system comprised from tubular work - piece heated by induction*. XXXI IC SPETO, Gliwice 2008, pp. 27-28.
- [10] Piątek Z., Szczegieliński T.: *Analiza numeryczna pola magnetycznego we wsadzie rurowym nagrzewanym indukcyjnie od wewnątrz*. Przegląd Elektrotechniczny, R.85, Nr 3/2009, ss. 63-66.
- [11] Kolańska-Płuska J.: *The Application of FEMM Program for Numerical Analysis of Electromagnetic Field of Rectangle Wires Section in Long Iron Pipes Hardening Process*. XXXII IC SPETO, Gliwice 2009, pp. 31-32.
- [12] Kurbiel A., Waradzyn Z.: *A method for Determining Electrical Quantities in a Workpiece Heated by Induction*. Electrical Power Quality and Utilisation, Vol. IX, No 1/2003, pp. 103-108.
- [13] Chiampi M., Chiarabaglio D., Tartaglia M.: *A general approach for analyzing power busbar under AC conditions*. IEEE Trans. on Magn., Vol. 29, No. 6, November 1993, pp. 2473-2475.
- [15] Du J., Burnett J., Fu Z. C.: *Experimental and numerical evaluation of busbar trunking impedance*. Electric Power Systems Research 55 (2000), pp. 113-119.
- [16] Cher R., Bryant J.: *The inductance of busbars of rectangular cross-section*. Australian Postmaster-General's Department: Research Laboratory Report No. 4139, February 1956.
- [17] Kalantarov P. L., Ciejtlin L. A.: *Calculating of inductances* (in Russian). Energija, Saint Petersburg 1970.
- [18] Strunskij B. M.: *Short electric network of electric furnaces* (in Russian). GN-TIL po Cz. i CM, Moscow 1962.
- [19] Au A., Maksymiuk J., Pochanke Z.: *Podstawy obliczeń aparatów elektroenergetycznych*. WNT, Warszawa 1982.
- [20] Grover F. W.: *Inductance Calculations*. Dover Phoenix Editions, New York 2004.
- [21] Battauscio O., Chiampi M., Chiarabaglio D.: *Experimental validation of a numerical model of busbar systems*. IEE Proc. Gener. Transm. Distrib., Vol. 142, No. 1, January 1995, pp. 65-72.
- [22] Dawson F. P., Cao M., Jain P. K.: *A simplified approach to calculating current distribution in paralleled busses*. IEEE Trans. Magn., Vol. 26, No. 2, 1990, 971-974.
- [23] Kazakov M. K.: *Using the full current law in discrete form for measuring high direct currents*. Electrical technology, No. 3, 1997, pp. 143-157.
- [24] Hwang C. C., Chang J. J., Jiang Y. H.: *Analysis of electromagnetic and thermal fields for a bus duct system*. Electric Power Systems Research 45 (1998), pp. 39-45.
- [25] Tozoni O. W., Kolerowa T. Ja.: *Multiphase industrial busducts*. Naukowa Dumka, Kiev 1966.
- [26] Du Y., Burnett J., Fu Z. C.: *Experimental and Numerical Evaluation of Busbar Trunking Impedance*. Electric Power Systems Research, No 55, 2000, pp. 113-119.
- [27] Lipiński W.: *Analiza rozkładu gęstości prądu w wydłużonej szynie prostokątnej*. Archiwum Elektrotechniki, tom XXIII, z. 1, 1974, ss. 49-57.
- [28] Piątek Z.: *Indukcyjność przewodu o przekroju prostokątnym i dowolnej długości*. Przegląd Elektrotechniczny, ISSN 0033-2097, R. 83, NR 2/2007, ss. 119-122.
- [29] Piątek Z.: *Zastosowanie równania całkowitego do wyznaczenia impedancji własnej przewodu szynowego dowolnej długości o przekroju prostokątnym*. X Konferencja "Zastosowania komputerów w elektrotermii" ZKwE 2006, Poznań, 18-20.04.2006, ss. 81-82.
- [30] Piątek Z., Kusiak D.: *The magnetic field intensity in a busbar of a rectangular cross-section with a finite length*. XXX International Conference on Fundamentals of Electrotechnics and Circuit Theory (XXX IC SPETO'2007), Gliwice – Ustroń, pp. 249-250.
- [31] Piątek Z., Kusiak D.: *The busbar of a rectangular cross-section - the magnetic field*. International Conference on Advance Methods in the Theory of Electrical Engineering Applied to Power Systems AMTEE'07, September 10-14 2007, Pilsen, Czech Republic, pp. 1.23-1.24.
- [32] Piątek Z., Kusiak D.: *Application of an integral equation for calculation of the impedance of any length busbar of rectangular cross-section*. ALWERS, ISBN 13: 978-83-923978-2-3, Poznań 2006, pp. 236-242.
- [33] Baron B., Kolańska-Płuska J.: *Application of Bessel functions and discrete Fourier transform to the analysis of electromagnetic system comprised of conducting solid or annular cylinder and coil wound it*. Prace Naukowe Politechniki Śląskiej, Seria Elektryka Nr 2(206) Politechnika Śląska, Gliwice 2008, pp. 33-52.
- [34] Krakowski M.: *Elektrotechnika teoretyczna. Pole Elektromagnetyczne*. WN PWN, Warszawa 1995.

*Authors: prof. nadzw. dr hab. inż. Jerzy Barglik: Politechnika Śląska, Wydział Inżynierii Materiałowej i Metalurgii, Katedra Zarządzania i Informatyki, ul. Krasińskiego 8, 40-019 Katowice, E-mail: jerzy.barglik@polsl.pl;
prof. dr hab. inż. Bernard Baron: Politechnika Śląska, Wydział Elektrotechniczny, Instytut Elektrotechniki Teoretycznej i Przemysłowej, Zakład Teorii Elektrotechniki, ul. Akademicka 10, 44-101 Gliwice, E-mail: bernard.baron@polsl.pl
dr inż. Joanna Kolańska-Płuska: Politechnika Opolska, Wydział Elektrotechniki Automatyki i Informatyki, Instytut Układów Elektromechanicznych i Elektroniki Przemysłowej, 45-036 Opole, ul. Luboszycka 7, E-mail: j.kolanska-pluska@po.opole.pl;
prof. dr hab. inż. Zygmunt Piątek: Politechnika Częstochowska, Wydział Inżynierii i Ochrony Środowiska, Instytut Inżynierii Środowiska, ul. Brzeźnicka 60a, 42-200 Częstochowa, E-mail: zygmunt.piatek@interia.pl;*